

# Demonstration of the ethylmalonyl-CoA pathway by using $^{13}\text{C}$ metabolomics

Rémi Peyraud<sup>a</sup>, Patrick Kiefer<sup>a</sup>, Philipp Christen<sup>a</sup>, Stephane Massou<sup>b</sup>, Jean-Charles Portais<sup>b,c</sup>, and Julia A. Vorholt<sup>a,1</sup>

<sup>a</sup>Institute of Microbiology, Eidgenössische Technische Hochschule Zurich, 8093 Zurich, Switzerland; <sup>b</sup>Unité Mixte de Recherche 5504, Unité Mixte de Recherche 792, Ingénierie des Systèmes Biologiques et des Procédés, Centre National de la Recherche Scientifique, Institut National de la Recherche Agronomique, Institut National des Sciences Appliquées, 31400 Toulouse, France; and <sup>c</sup>Faculté Sciences de la Vie Université Paul Sabatier, 31062 Toulouse, France

Edited by Hans Kornberg, Boston University, Boston, MA, and approved January 8, 2009 (received for review October 31, 2008)

The assimilation of one-carbon (C1) compounds, such as methanol, by serine cycle methylotrophs requires the continuous regeneration of glyoxylate. Instead of the glyoxylate cycle, this process is achieved by a not yet established pathway where CoA thioesters are known to play a key role. We applied state-of-the-art metabolomics and  $^{13}\text{C}$  metabolomics strategies to demonstrate how glyoxylate is generated during methylotrophic growth in the isocitrate lyase-negative methylotroph *Methylobacterium extorquens* AM1. High-resolution mass spectrometry showed the presence of CoA thioesters specific to the recently proposed ethylmalonyl-CoA pathway. The operation of this pathway was demonstrated by short-term  $^{13}\text{C}$ -labeling experiments, which allowed determination of the sequence of reactions from the order of label incorporation into the different CoA derivatives. Analysis of  $^{13}\text{C}$  positional enrichment in glycine by NMR was consistent with the predicted labeling pattern as a result of the operation of the ethylmalonyl-CoA pathway and the unique operation of the latter for glyoxylate generation during growth on methanol. The results also revealed that 2 molecules of glyoxylate were regenerated in this process. This work provides a complete pathway for methanol assimilation in the model methylotroph *M. extorquens* AM1 and represents an important step toward the determination of the overall topology of its metabolic network. The operation of the ethylmalonyl-CoA pathway in *M. extorquens* AM1 has major implications for the physiology of these methylotrophs and their role in nature, and it also provides a common ground for C1 and C2 compound assimilation in isocitrate lyase-negative bacteria.

$^{13}\text{C}$  labeling | CoA ester | methylotroph | one-carbon metabolism | glyoxylate regeneration

Methylotrophic bacteria are organisms capable of using reduced carbon compounds, such as methanol or methane, as sole sources of carbon and energy, and they play a key role in carbon cycling in their environment. They also represent promising organisms in biotechnology for the conversion of one-carbon (C1) substrates to value-added products (1). The elucidation of the mechanisms enabling growth on reduced C1 compounds of *Methylobacterium extorquens* AM1, one of the most studied methylotrophs, has been a longstanding goal, and although great progress has been made (2–5), it is still not fully achieved. A key point has been to understand how the bacterium incorporates C1 units into cell material. The serine cycle was elucidated in this organism during the early 1960s by Quayle and coworkers (6–9). The assimilation of C1 units by this pathway requires continuous regeneration of glyoxylate from acetyl-CoA and can be achieved, in principle, via the well-known glyoxylate cycle (10). However, Dunstan and coworkers (11–14) showed in 1972 and 1973 that *M. extorquens* AM1 lacks the key enzyme of the glyoxylate cycle, isocitrate lyase, but has an alternative route involving oxidation of acetate to glyoxylate that functions during growth on both C1 and C2 compounds. Also, other organisms, including the photosynthetic *Rhodospirillum rubrum* are known to require an alternative to the glyoxylate cycle when growing on C2 substrates or on substrates that are converted into acetyl-CoA to enter central metabolism (15–18).

Recent studies, including mutant analyses, gene predictions, enzyme assays, and metabolite studies in *M. extorquens* AM1, have led to the observation that a complex sequence of CoA thioester derivatives is involved in glyoxylate regeneration, resulting in the hypothesis of the so-called glyoxylate regeneration cycle (GRC) (19, 20) [Fig. 1 and supporting information (SI) Table S1]. According to this pathway, a C5 compound, methylsuccinyl-CoA, is formed from the condensation of 2 acetyl-CoA molecules plus 1  $\text{CO}_2$  and is decarboxylated twice in a process similar to valine degradation. The specific intermediates of the GRC are isobutyryl-CoA, metacrylyl-CoA, and hydroxyisobutyryl-CoA, and the result is the formation of propionyl-CoA. Subsequently, propionyl-CoA is transformed to malate, from which 1 glyoxylate and 1 acetyl-CoA are generated (20). More recently, a second hypothesis, the ethylmalonyl-CoA pathway (EMCP), was proposed from studies of C2 assimilation pathways in *R. sphaeroides* (21–23). This pathway (Fig. 1 and Table S1) includes the formation of methylsuccinyl-CoA, which is further converted to methylmalyl-CoA, from which both glyoxylate and propionyl-CoA are released by cleavage (22). The propionyl-CoA can then be converted to C4 compounds and assimilated as cell material (23).

The 2 pathways mentioned above are still hypothetical, and none has been firmly demonstrated to operate in vivo. They differ strikingly in terms of carbon balance and, therefore, overall carbon yield for methylotrophic growth. The GRC includes a net decarboxylation step, whereas the ethylmalonyl-CoA pathway includes net carboxylation steps. This makes the second pathway more efficient in terms of carbon assimilation and has important implications with regard to the physiology of these methylotrophs and their actual biotechnological potential.

In this work, we combined state-of-the-art metabolomics and  $^{13}\text{C}$  metabolomics strategies to examine the pathway of glyoxylate regeneration occurring in *M. extorquens* AM1 under methylotrophic conditions. The development of an original liquid chromatography high-resolution mass spectrometry (LC-HRMS) method allowed for the identification of almost all intermediates of the ethylmalonyl-CoA pathway. Detailed and conclusive information regarding the operation of the ethylmalonyl-CoA pathway as the predominant process for glyoxylate formation was obtained from  $^{13}\text{C}$ -labeling experiments in which kinetic isotopomer profiles collected by LC-HRMS during short-term  $^{13}\text{C}$ -labeling experiments were combined with steady-state isotopomer distributions measured by NMR.

## Results

**Identification of CoA Thioesters by Liquid Chromatography-Mass Spectrometry (LC-MS).** The pathways proposed for the conversion of acetyl-CoA to glyoxylate in isocitrate lyase-negative bacteria involve

Author contributions: R.P., P.K., J.-C.P., and J.A.V. designed research; R.P., P.K., P.C., and S.M. performed research; P.K. and S.M. contributed new reagents/analytic tools; R.P., P.K., S.M., and J.-C.P. analyzed data; and R.P., J.-C.P., and J.A.V. wrote the paper.

The authors declare no conflict of interest.

This article is a PNAS Direct Submission.

<sup>1</sup>To whom correspondence should be addressed. E-mail: vorholt@micro.biol.ethz.ch.

This article contains supporting information online at [www.pnas.org/cgi/content/full/0810932106/DCSupplemental](http://www.pnas.org/cgi/content/full/0810932106/DCSupplemental).



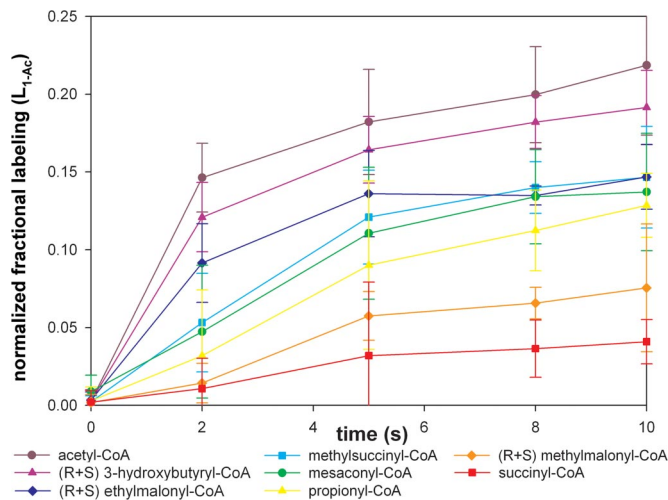


**Fig. 4.** Kinetics of  $^{13}\text{C}$  label incorporation in CoA thioesters after addition of  $[1-^{13}\text{C}]\text{acetate}$  to  $[2-^{13}\text{C}]\text{methanol}$ -grown *M. extorquens* AM1 cells.  $\text{L}_{1-\text{Ac}}$  represents the percent of  $^{13}\text{C}$  label incorporated in a given metabolite, normalized to the maximal number of carbon atoms received from the first carbon of acetate. Results are mean values + SDs from 3 independent biological replicates.

propionyl-CoA was essentially indistinguishable from that of the 2 C5 CoA thioesters, methylsuccinyl-CoA and mesaconyl-CoA, indicates that no loss of labeled carbon occurred. After propionyl-CoA, methylmalonyl-CoA was found to be labeled, followed by succinyl-CoA. Their isotopomer profiles were similar to those of metabolites in the early steps of the pathway, indicating that they are all connected through the same sequence of reactions.

After 10 s of incubation, the percentage of  $^{13}\text{C}$  label incorporated into ethylmalonyl-CoA did not increase further, unlike other CoA metabolites (Fig. 4). Further investigations are needed to understand this observation. However, the mass isotopomer distribution (relative proportions of M0, M+1, M+2, etc.) of ethylmalonyl-CoA remained constant over time, suggesting that the process by which the label was transferred from [ $^{13}\text{C}$ ]acetate to this metabolite did not change during the incubation period.

The mass isotopomers of few CoA intermediates were difficult to quantify because of small pool sizes. Therefore, replicate samples collected at the same time points were pooled and concentrated. The concentrated samples indicated that crotonyl-CoA was labeled similarly to 3-hydroxybutyryl-CoA and before butyryl-CoA and ethylmalonyl-CoA. Butyryl-CoA was found to be labeled more than ethylmalonyl-CoA and similarly to methylsuccinyl-CoA.  $\beta$ -methylmalyl-CoA was labeled before the other C5 compounds mentioned above and with a high level of M+2, which supposes an incorporation of label from mesaconyl-CoA plus an entry of label from glyoxylate due to the reversibility of the reaction catalyzed by L-malyl-CoA/ $\beta$ -methylmalyl-CoA lyase (22, 24).

Taken together, the label incorporation in CoA thioesters is in agreement with the sequence of reactions shown in Fig. 1 and suggests the operation of the ethylmalonyl-CoA pathway (23).

**Mass Isotopomers of Propionyl-CoA.** Because the fate of carbon atoms derived from [1-<sup>13</sup>C]acetate is different in the 2 proposed pathways, the generated propionyl-CoA molecules do not receive the same number of carbon atoms; i.e., doubly labeled M+2 propionyl-CoA would be formed according to the ethylmalonyl-CoA pathway (Fig. 3), whereas only singly labeled M+1 propionyl-CoA would be formed according to the GRC as a result of carbon loss as CO<sub>2</sub>. Examination of the evolution of the mass isotopomer distribution of propionyl-CoA during [1-<sup>13</sup>C]acetate-labeling experiments showed increases of M+2 until  $24.1\% \pm 2.6\%$  at 90 s of

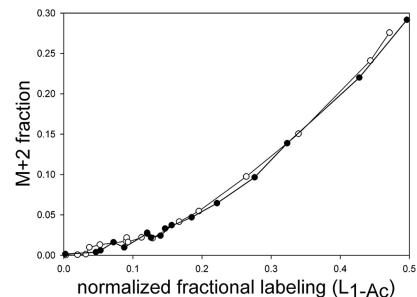


**Fig. 5.** Comparison of the time course evolution of M+2 isotopomeric fractions in propionyl-CoA (○) and methylsuccinyl-CoA (●) during [1-<sup>13</sup>C]acetate labeling experiments carried out with methanol-grown *M. extorquens* AM1 cells. The parallel development of the M+2 fraction in the 2 metabolites indicated that no loss of carbon occurred in the process by which methylsuccinyl-CoA was converted to propionyl-CoA.

incubation time. To determine whether a decarboxylation step operates between methylsuccinyl-CoA and propionyl-CoA, the proportion of M+2 isotopomers in methylsuccinyl-CoA and propionyl-CoA during the entire labeling experiment was compared (Fig. 5). The proportion was found to be the same, indicating that no decarboxylation reaction occurred, as would have been observed if the GRC was operating under our experimental conditions.

**Analysis of Glycine Isotopomers Generated from [ $^{13}\text{C}$ ]Methanol Under Pure Methylophilic Conditions.** To examine the contribution of the ethylmalonyl-CoA pathway to glyoxylate regeneration under pure methylophilic conditions, a model of glyoxylate metabolism was built up to simulate the theoretical fate of carbon in the central metabolic network (serine cycle, glyoxylate regeneration, and citric acid cycle) of *M. extorquens* AM1 from [ $^{13}\text{C}$ ]methanol and  $\text{CO}_2$  at natural abundance. This model was used to calculate the steady-state isotopomer distribution in glyoxylate expected to occur when each pathway (either GRC or EMCP) was considered separately (for information on underlying considerations and results, see Fig. S1). By operation of the GRC (20), the 2 major isotopomers are expected to be  $^{12}\text{C}_1\text{-}^{13}\text{C}_2$  and  $^{13}\text{C}_1\text{-}^{12}\text{C}_2$ , and they should represent 41.1% and 33.3%, respectively, of all glyoxylate isotopomers (Table 1). According to the ethylmalonyl-CoA pathway (23), the 2 major isotopomers are expected to be  $^{12}\text{C}_1\text{-}^{13}\text{C}_2$  and  $^{12}\text{C}_1\text{-}^{12}\text{C}_2$ , and their steady-state proportions should represent 57.1% and 39.1%, respectively, of all glyoxylate isotopomers (Table 1). Taken together, the results of these simulations revealed that the 2 pathways result in strongly discriminative labeling patterns in glyoxylate.

Notably, Large et al. (7) in 1962 used  $^{14}\text{C}$ -labeling strategies to investigate the serine cycle in *M. extorquens*. They found disproportionate labeling, in which 92.5% of the label from  $[^{14}\text{C}]$ methanol incorporated into glycine was recovered in the C2 position. Although these results found almost half a century ago were not interpreted in that way, they are consistent with the operation of the ethylmalonyl-CoA pathway (23) (Table 1). This seminal study, however, did not provide detailed measurement of the various isotopomers from which conclusive information regarding the operation of the 2 pathways could be obtained.

To obtain more detailed labeling information, we analyzed by NMR the positional isotopomers of glycine. Data were generated during steady-state  $^{13}\text{C}$ -labeling experiments carried out with  $^{13}\text{C}$ -enriched methanol and  $\text{CO}_2$  at natural abundance, so that the labeling of free glycine—and glyoxylate—could be measured from the more abundant proteinogenic glycine. The 4 positional isotopomers of glycine were measured by combining 2D ZQF-TOCSY and 2D-HSQC experiments (25, 26) (Table S3 and Fig. S2). The results obtained for 3 biological replicates are shown in Table 1. The fractional enrichments (percentages of label in the carbon position)



**Table 1. Steady-state distribution of  $^{13}\text{C}$  labeling in glycine in *M. extorquens* AM1 during methylotrophic growth on  $^{13}\text{C}$ methanol**

	Predicted data according to		Experimental data	
Isotopomer	GRC	EMCP	This study	Large et al. (7)
Isotopomer distribution (% of total glycine isotopomers)				
<sup>12</sup> C <sup>1</sup> - <sup>12</sup> C <sup>2</sup>	18.4	39.1	32.3 ± 0.7	
<sup>13</sup> C <sup>1</sup> - <sup>12</sup> C <sup>2</sup>	33.3	2.8	2.0 ± 1.0	
<sup>12</sup> C <sup>1</sup> - <sup>13</sup> C <sup>2</sup>	41.1	57.1	60.1 ± 2.9	
<sup>13</sup> C <sup>1</sup> - <sup>13</sup> C <sup>2</sup>	7.2	1.0	5.6 ± 2.0	
Label recovery (% of total label in glycine)				
C <sup>1</sup>	45.6	6.2	10.4 ± 4.0*	7.5
C <sup>2</sup>	54.4	93.8	89.6 ± 6.6*	92.5

Experimental data were obtained from NMR data recorded on proteinogenic amino acids of *M. extorquens* AM1 growing on [ $^{13}\text{C}$ ]methanol and 5%  $\text{CO}_2$  at natural abundance. The distribution of glycine isotopomers expected from the pure operation of either the GRC (20) or EMCP (23) was calculated from a mathematical model taking into account the stoichiometry and the carbon atom transition of each process. The percentage of  $^{13}\text{C}$  label recovered in the 2 carbon positions of glycine (Experimental data) were compared with the values of  $^{14}\text{C}$ -label recovery in intracellular glycine measured by Large et al. (7) and to the values predicted.

\*Correlated value.

of C1 and C2 were 7.6% and 65.7%, respectively, indicating that  $89.6 \pm 6.6\%$  of the  $^{13}\text{C}$  label was recovered in the C2 position in our experiments. The latter value is closely similar to the 92.5% determined by Large et al. (7) in 1962.

The steady-state distribution of [ $^{13}\text{C}$ ]isotopomers in glycine (Table 1) was used to determine the metabolic origin of glyoxylate in *M. extorquens* AM1 under pure methylotrophic conditions. The relative flux distributions calculated are displayed in Fig. 6. The steady-state positional isotopomers of glycine were consistent with the almost unique operation of the ethylmalonyl-CoA pathway (flux relative to methanol uptake:  $25\% \pm 1\%$ ), because the contribution of the GRC, if any, was within the limits of experimental errors ( $0\% \pm 2\%$ ). The apparent discrepancy between the observed isotopic pattern of glyoxylate (Table 1) and the theoretical

expectations for the pure operation of the ethylmalonyl-CoA pathway could be explained by the contribution of  $^{13}\text{C}$   $\text{CO}_2$  produced by methanol oxidation. The culture was aerated with 5%  $\text{CO}_2$  to remove the  $^{13}\text{C}$   $\text{CO}_2$  produced by the bacteria. Under this condition, 6%  $\text{CO}_2$  was found to come from methanol oxidation. Moreover, all isotopomer constraints were satisfied in the calculations, suggesting that if any other pathway contributed to glyoxylate formation, it would result in the same labeling patterns as those induced by the metabolic pathways considered.

The data shown in Fig. 6 allowed us to calculate the contribution of the various pathways to glyoxylate biosynthesis. For each turn of the serine cycle, 25% of glyoxylate molecules were regenerated by direct cleavage of methylmalyl-CoA, whereas the remaining 75% were obtained from malate. Of these 75%,  $\approx 50\%$  corresponded to malate recycled in the serine cycle, and the remaining 25% were generated from the propionyl-CoA molecules generated in the ethylmalonyl-CoA pathway. This indicated that the proportion of glyoxylate molecules regenerated from propionyl-CoA (25%) was in the range of that generated directly from the cleavage of methylmalyl-CoA (25%). These data were consistent with the wide majority of propionyl-CoA molecules generated in the ethylmalonyl-CoA pathway being used for the regeneration of glyoxylate.

## Discussion

The present study shows that glyoxylate regeneration in *M. extorquens* AM1 occurs by the ethylmalonyl-CoA pathway (23). This conclusion was drawn from: (i) examination of the CoA thioesters present in cells during growth on methanol, (ii) kinetics of label incorporation in these CoA thioesters during short  $^{13}\text{C}$ -labeling experiments, and (iii) steady-state  $^{13}\text{C}$ -labeling experiments providing quantitative information with regard to the metabolic origin of glyoxylate carbon atoms, which essentially rule out a contribution of the GRC.

The original LC-MS method developed here for direct analysis of the CoA thioesters proved to be critical to demonstrate the occurrence of specific intermediates of the ethylmalonyl-CoA pathway and to determine the sequence of reactions. It provides an analytical platform for the analysis of a large number of CoA thioesters, which are of broad interest not only for the study of methylo-trophy but also for other metabolic purposes, such as CO<sub>2</sub> assimilation in autotrophs (27), fatty acid and polyketide metabolisms, and bioremediation/degradation of aromatic compounds and hydrocarbons (28, 29). The present work also emphasizes the complementarities of MS and NMR to resolve the topology of complex metabolic networks from <sup>13</sup>C-labeling experiments. The present work demonstrates that the combination of the 2 methods is highly valuable, because the (increasing) sensitivity of mass spectrometers allows short-term labeling experiments to be carried out, resulting in dynamic information on a given metabolic network, whereas NMR is unique in providing detailed positional labeling information from which metabolic pathways can be directly identified and quantified.

The sequence of reactions that converts acetyl-CoA into glyoxylate observed in *M. extorquens* AM1 in vivo is in agreement with that proposed for *R. sphaeroides* (23), where crotonyl-CoA is converted into ethylmalonyl-CoA by the crotonyl-CoA reductase/carboxylase (23). The data do not rule out that this conversion could occur also via butyryl-CoA (20) and its carboxylation by propionyl-CoA carboxylase (Fig. 1), although the recent demonstration that crotonyl-CoA reductase/carboxylase is present in methanol-grown *M. extorquens* makes the former process more likely (23). In any case, the pathway converts 2 acetyl-CoA molecules into glyoxylate and succinyl-CoA, and the carbon balance of the process is:

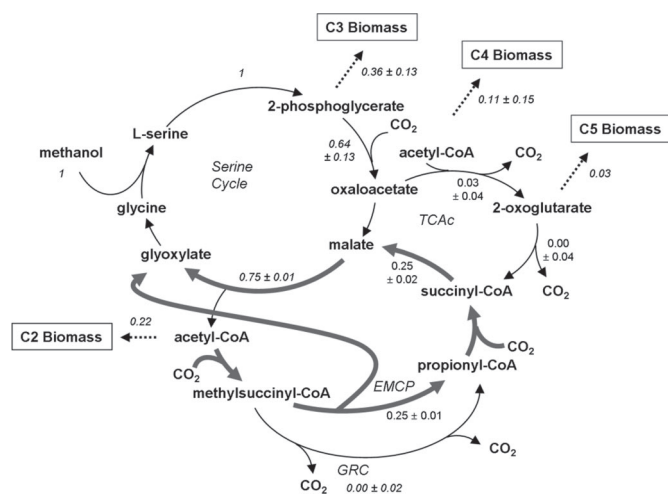
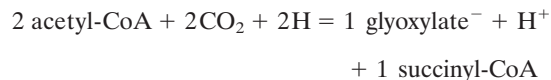


**Fig. 6.** Metabolic origin of glyoxylate in *M. extorquens* AM1 during growth on methanol. The contributions of central metabolic pathways to glyoxylate biosynthesis were calculated from the positional isotopomers of glycine measured by NMR. Results are expressed relative to methanol uptake, set arbitrarily to 1.0, and confidence intervals are given within brackets. TCA indicates tricarboxylic acid cycle; EMCP, ethylmalonyl-CoA pathway (23); and GRC, glyoxylate regeneration cycle (20).

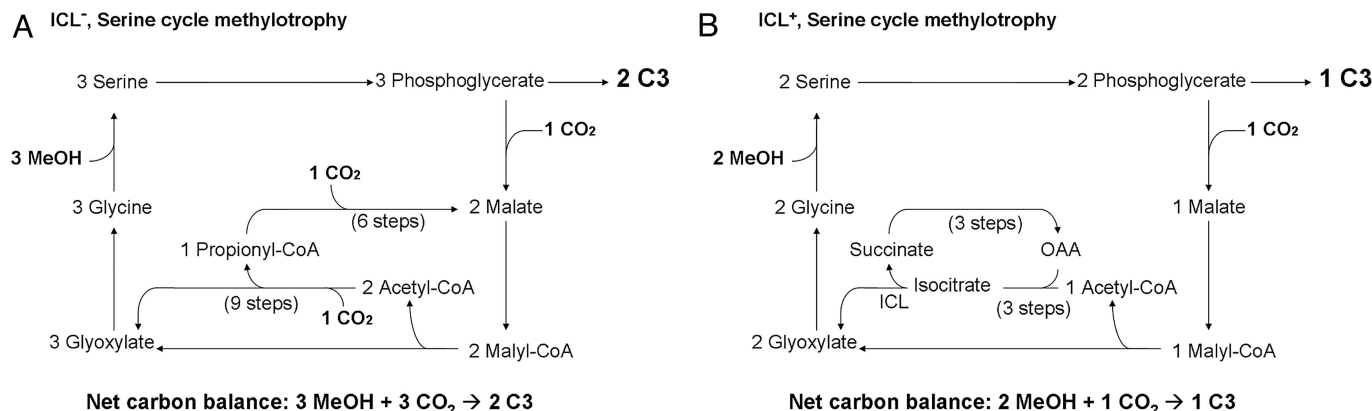
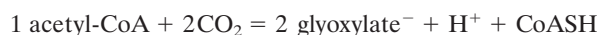


**Fig. 7.** Comparison of C1 assimilation pathways in isocitrate lyase-negative (ICL<sup>-</sup>; A), proposed from this study, and positive (ICL<sup>+</sup>; B) serine cycle methylotrophs. Note that CO<sub>2</sub> is derived from methanol, and therefore the overall carbon balance is the same in the 2 organisms: 3 methanol → 1 C<sub>3</sub>.

This balance highlights the occurrence of 2 net carboxylation steps in the ethylmalonyl-CoA pathway, which is different not only from the GRC, where carbon loss would occur, but also from the classical glyoxylate cycle (10), where no carboxylation occurs.

The operation of the ethylmalonyl-CoA pathway has major implications for C1 assimilation in *M. extorquens* AM1 in terms of carbon balance and metabolic organization. The carbon balance of the whole process of C1 assimilation depends on the behavior of the succinyl-CoA molecule generated along with glyoxylate in the ethylmalonyl-CoA pathway. Erb et al. (23) proposed that succinyl-CoA was directly incorporated into cell material; however, the labeling data collected here for pure methylotrophic growth conditions indicate that succinyl-CoA is used to regenerate glyoxylate. Moreover, the positional isotopomers of glycine measured by NMR were consistent with a significant contribution of this process to glyoxylate regeneration, because the proportion of glyoxylate molecules regenerated from propionyl-CoA was calculated to be similar to that released by the cleavage of methylmalyl-CoA. These results indicate that not only 1 but 2 molecules of glyoxylate are regenerated by the ethylmalonyl-CoA pathway in *M. extorquens* AM1, with the following carbon balance:



The demonstration of the ethylmalonyl-CoA pathway closes the serine cycle during methylotrophic growth, a problem that has been unsolved since 1963 (9). The mechanism of C1 assimilation resulting from our observations (Fig. 6) shows that 2 molecules of glyoxylate can be regenerated at the same time. It also provides the molecular basis for the explanation of labeling data showing that roughly half the biomass carbon comes from CO<sub>2</sub> during methylotrophic growth conditions under laboratory conditions (6, 30). Therefore, the oxidation of methanol into CO<sub>2</sub> occurring in the initial steps of methanol utilization appears to be critical not only for energy purposes but also for carbon assimilation. A comparison of the carbon balance in ICL-negative and ICL-positive serine cycle methylotrophs (Fig. 7) reveals that the former organisms have a higher CO<sub>2</sub> fixation ability than the latter, although the energetic cost is likely to be higher as well. The high efficiency of carbon recovery during methylotrophic growth has major implications for the physiology of these widespread organisms and for their role in carbon cycling in their environment, and it poses questions as to what extent CO<sub>2</sub> is recycled from endogenously formed methanol or the atmosphere under natural conditions.

## Materials and Methods

**Reagents, Medium Composition, and Culture Conditions.** [<sup>13</sup>C]methanol (99%) and [<sup>12</sup>C]methanol (99.9%) were purchased from Cambridge Isotope Laboratories; D<sub>2</sub>O (99.8% and 99.97%) were purchased from Eurisotop. All other chemicals

were purchased from Sigma. Acetonitrile, formic acid, and ammonium used for HPLC solvents were of LC-MS degree. *M. extorquens* AM1 was grown on minimal medium containing 1.62 g/L NH<sub>4</sub>Cl, 0.2 g/L MgSO<sub>4</sub>, 2.21 g/L K<sub>2</sub>HPO<sub>4</sub>, 1.25 g/L NaH<sub>2</sub>PO<sub>4</sub>·2H<sub>2</sub>O, and the following trace elements: 15 mg/L Na<sub>2</sub>EDTA·2H<sub>2</sub>O, 4.5 mg/L ZnSO<sub>4</sub>·7H<sub>2</sub>O, 0.3 mg/L CoCl<sub>2</sub>·6H<sub>2</sub>O, 1 mg/L MnCl<sub>2</sub>·4H<sub>2</sub>O, 1 mg/L H<sub>3</sub>BO<sub>3</sub>, 2.5 mg/L CaCl<sub>2</sub>, 0.4 mg/L of Na<sub>2</sub>MoO<sub>4</sub>·2H<sub>2</sub>O, 3 mg/L FeSO<sub>4</sub>·7H<sub>2</sub>O, and 0.3 mg/L CuSO<sub>4</sub>·5H<sub>2</sub>O. All batch cultures were carried out in a 500-mL bioreactor (Infors-HT) at 28 °C and at 1000 rpm. The pH was kept constant at 7.0 by addition of 1 M NH<sub>4</sub>OH. For the purpose of short-term <sup>13</sup>C-labeling experiments, cells were grown in 300 mL of medium containing 0.5% <sup>13</sup>C-depleted methanol, and were aerated with compressed air at 0.15 L/min. Initial optical density (OD<sub>600</sub>) was 0.2, and sampling was performed between ODs 2.8 and 3.0. Cultures carried out for the purpose of steady-state labeling experiments were grown in 400 mL of medium containing [<sup>13</sup>C]methanol and aerated with synthetic air containing 5% natural labeled CO<sub>2</sub>. To keep the fraction of dissolved <sup>13</sup>C-CO<sub>2</sub> produced from methanol below 2%, aeration rate was increased as follows: 0.2 L/min until OD 0.6, 0.4 L/min until OD 1, and 0.6 L/min until sampling. Initial OD was 0.01, and cells were harvested at around OD 1.5.

**Sampling and Extraction of CoA Thioesters.** A total of 1 mL of culture corresponding to 0.6 mg of cell dry weight was directly transferred into 4.5 mL of 95% acetonitrile at -20 °C containing 25 mM formic acid for quenching. To provide instantaneous quenching of metabolic activity, the sample was added into the quenching solution on a Vortex. Cells were disrupted by 3 sonication steps (30 s, 23 kHz) by using a Soniprep 150 device (Sanyo) and carried out in a cooling bath (T < -10 °C), with 30 s between each treatment. After the addition of 20 mL of ice-cold H<sub>2</sub>O, the sample was chilled with liquid nitrogen. Frozen samples were stored at -20 °C until freeze drying. Subsequently, 300 μL of an ice-cold, 25 mM ammonium formate buffer (pH 3.5, 2% MeOH) was added. The suspension was centrifuged (14,000 × g, 2 min, -5 °C), and the supernatant was filtered through a Sartorius Minisart filter (pore size 0.2 μm) before analysis.

**LC-MS Analysis.** Analyses were performed with a Rheos 2200 HPLC system (Flux Instruments) coupled to an LTQ Orbitrap mass spectrometer (Thermo Fisher Scientific), equipped with an electrospray ionization probe. CoA esters were separated with a C<sub>18</sub> analytical column (Gemini 150 × 2.0 mm, particle size 3 μm; Phenomenex) at a flow rate of 220 μL min<sup>-1</sup>. Injection volume was 10 μL. Solvent A was 50 mM formic acid adjusted to pH 8.1 with NH<sub>4</sub>OH, and solvent B was methanol. The following gradient of B was applied: 0 min, 5%; 1 min, 5%; 10 min, 23%; 20 min, 80%; 22 min, 80%. MS analysis was done in the negative FTMS mode at a resolution of 15,000 (*m/z* = 400) to determine mass isotopomer distribution patterns and at a resolution of 60,000 (*m/z* = 400) to identify CoA thioesters and to detect potential mass peak overlapping problems. Sheath gas flow rate was 40, aux gas flow rate was 10, tube lens was -90 V, capillary voltage was -4 V, and ion spray voltage was -4.7 kV.

For the identification of CoA thioesters in cell extracts, chromatograms were analyzed for the presence of [M-H]<sup>-</sup> ions corresponding to the exact mass expected from the 15 CoA thioesters potentially involved in glyoxylate regeneration, with a mass tolerance of 5 ppm. The number of carbon atoms was validated by using additional extracts from *M. extorquens* cells grown on [<sup>13</sup>C]methanol.

**Short-Term <sup>13</sup>C-Labeling Experiments.** Incubation of cells with labeled acetate was realized in 2-mL Eppendorf tubes containing 50 μL of 1.05 M [1-<sup>13</sup>C]acetate.

To start, 1 mL of culture growing on [ $^{12}\text{C}$ ]methanol was quickly added with a syringe in the Eppendorf tube, and the sample was vortexed. A final acetate concentration of 50 mM was chosen to reach the same concentration as methanol. The acetate homogenization time in the final sample was found to be  $1.1 \pm 0.2$  seconds. After various incubation times, the solution was added to the quenching solution, and the CoA thioesters were analyzed as explained above. The efficiency of the quenching process was evaluated by examining label incorporation into CoA thioesters in a culture sample injected in the quenching solution containing [ $^{13}\text{C}$ ]acetate without an incubation period and revealing no incorporation of label.

**Calculations of Normalized  $^{13}\text{C}$ -Label Incorporation.** The incorporation of  $^{13}\text{C}$  label in each CoA ester during short-term  $^{13}\text{C}$ -labeling experiments was calculated from the analysis of the corresponding isotopic cluster in the mass spectra. The data were corrected for naturally occurring isotopes, the contribution of which was determined from the analysis of samples collected just before the addition of [ $^{13}\text{C}$ ]acetate. Results are expressed as percent of  $^{13}\text{C}$  atoms incorporated in the molecule. Because the different CoA esters do not receive the same number of  $^{13}\text{C}$  atoms from [ $^{13}\text{C}$ ]acetate, results were normalized according to the maximum number of  $^{13}\text{C}$  atoms that can be received from [ $^{13}\text{C}$ ]acetate in the considered molecule ("normalized fractional labeling,"  $L_{1-\text{Ac}}$ ):

$$L_{1-\text{Ac}} = \frac{\left( \sum_{i=1}^n M_i \times i \right)}{n}$$

Where  $M_i$  is the proportion of the mass isotopomer corresponding to molecules having incorporated  $i$   $^{13}\text{C}$  atoms from [ $^{13}\text{C}$ ]acetate;  $n$  is the maximum number of [ $^{13}\text{C}$ ]carbon that can be incorporated into the molecule from [ $^{13}\text{C}$ ]acetate (note that for some compounds,  $n$  is different according to GRC or EMCP).

**NMR Analyses.** All 1D and 2D NMR spectra were recorded on a Bruker Avance II 500-MHz spectrometer using a 5-mm z-gradient BBI probe head. The data were

acquired and processed by using TOPSPIN 1.3 software (Bruker). The temperature was 298 K. The 1D  $^1\text{H}$  spectra were acquired by using a  $30^\circ$  pulse, 5,000-Hz sweep width, and 3.27-s acquisition times. A total of 128 scans were recorded, and relaxation delay between scans was 10 s. Proteinogenic amino acid sample was prepared as described previously (25) and modified as explained in the *SI Text*. Positional isotopomers of proteinogenic glycine were measured from (i) the analysis of carbon-carbon couplings in 2D- $^{13}\text{C}$ -HSQC spectra and (ii) the analysis of heteronuclear  $^1\text{H}$ ,  $^{13}\text{C}$  couplings in 2D ZQF-TOCSY spectra (25, 26). The peak deconvolution was realized with the software GOSA-fit ([www.biol-log.biz/](http://www.biol-log.biz/)). The value of the glycine  $^2\text{J}_{\text{H}_2\text{C}_1}$  coupling constant was determined from the 1D  $^1\text{H}$  analysis of 0.45 M [ $^{13}\text{C}$ ,  $^{15}\text{N}$ ]glycine performed with and without COOH decoupling.

**Flux Calculations.** For the purpose of flux calculations, a reaction network describing C1 metabolism in *M. extorquens* AM1, including simplified reactions for biomass formation, was designed. This model described the stoichiometry of the reactions as well as the transitions of carbon atoms. Biomass requirements were obtained from Van Dien and Lidstrom (31). Relative flux distributions were calculated from the positional isotopomers of glycine collected by NMR using both the 13C-Flux software developed by Wiechert (32). Results are expressed as molar fluxes relative to the rate of methanol uptake (set arbitrarily to 1.0).

**ACKNOWLEDGMENTS.** We thank T. Erb (University of Freiburg, Freiburg, Germany) for the generous gift of several CoA standards, and S. Sokol (Institut National des Sciences Appliquées, Toulouse, France) for fruitful discussions and support in metabolic simulations. This work was supported by Eidgenössische Technische Hochschule Zurich Research Grant ETH-25 08-2. Evonik Degussa GmbH and North Rhine-Westphalia cofinanced by the European Union are acknowledged for supporting the development of LC-MS analytics. The Swiss Academy of Engineering Science (SATW) and the Centre Français pour l'Accueil et les Echanges Internationaux (Egide) supported the work with a travel grant (Germaine de Staël program). The work carried out at the Laboratory for BioSystems & Process Engineering (Toulouse, France) was supported by grants from the Agence Nationale de la Recherche, the Région Midi-Pyrénées, and the European Regional Development Fund (ERDF).

- Schrader J, et al. (2009) Methanol-based industrial biotechnology: Current status and future perspectives of methylotrophic bacteria. *Trends Biotechnol* 27:107–115.
- Anthony C (1982) *The Biochemistry of Methylotrophs* (Academic, London).
- Chistoserdova L, Vorholt JA, Thauer RK, Lidstrom ME (1998) C1 transfer enzymes and coenzymes linking methylotrophic bacteria and methanogenic Archaea. *Science* 281:99–102.
- Chistoserdova L, Chen SW, Lapidus A, Lidstrom ME (2003) Methylotrophy in *Methylobacterium extorquens* AM1 from a genomic point of view. *J Bacteriol* 185:2980–2987.
- Vorholt JA (2002) Cofactor-dependent pathways of formaldehyde oxidation in methylotrophic bacteria. *Arch Microbiol* 178:239–249.
- Large PJ, Peel D, Quayle JR (1961) Microbial growth on C1 compounds. II. Synthesis of cell constituents by methanol- and formate-grown *Pseudomonas* AM1, and methanol-grown *Hyphomicrobium vulgare*. *Biochem J* 81:470–480.
- Large PJ, Peel D, Quayle JR (1962) Microbial growth on C(1) compounds. 3. Distribution of radioactivity in metabolites of methanol-grown *Pseudomonas* AM1 after incubation with [ $^{14}\text{C}$ ]methanol and [ $^{14}\text{C}$ ]bicarbonate. *Biochem J* 82:483–488.
- Large PJ, Peel D, Quayle JR (1962) Microbial growth on C(1) compounds. 4. Carboxylation of phosphoenolpyruvate in methanol-grown *Pseudomonas* AM1. *Biochem J* 85:243–250.
- Large PJ, Quayle JR (1963) Microbial growth on C(1) compounds. 5. Enzyme activities in extracts of *Pseudomonas* AM1. *Biochem J* 87:386–396.
- Kornberg HL, Krebs HA (1957) Synthesis of cell constituents from C2-units by a modified tricarboxylic acid cycle. *Nature* 179:988–991.
- Dunstan PM, Anthony C, Drabble WT (1972) Microbial metabolism of C 1 and C 2 compounds. The involvement of glycolate in the metabolism of ethanol and of acetate by *Pseudomonas* AM1. *Biochem J* 128:99–106.
- Dunstan PM, Anthony C (1972) Microbial growth on C-1 and C2 compounds: The metabolism of acetate to glycine in *Pseudomonas* AM1. *Biochem J* 130:31P.
- Dunstan PM, Anthony C, Drabble WT (1972) Microbial metabolism of C1 and C2 compounds. The role of glyoxylate, glycolate and acetate in the growth of *Pseudomonas* AM1 on ethanol and on C1 compounds. *Biochem J* 128:107–115.
- Dunstan PM, Anthony C (1973) Microbial metabolism of C1 and C2 compounds. The role of acetate during growth of *Pseudomonas* AM1 on C1 compounds, ethanol and beta-hydroxybutyrate. *Biochem J* 132:797–801.
- Kornberg HL, Lascelles J (1960) The formation of isocitrate by the Athiorhodaceae. *J Gen Microbiol* 23:511–517.
- Albers H, Gottschalk G (1976) Acetate metabolism in *Rhodospseudomonas gelatinosa* and several other Rhodospirillaceae. *Arch Microbiol* 111:45–49.
- Han L, Reynolds KA (1997) A novel alternate anaplerotic pathway to the glyoxylate cycle in streptomycetes. *J Bacteriol* 179:5157–5164.
- Claassen PAM, Zehnder AJB (1986) Isocitrate lyase activity in *Thiobacillus versutus* grown anaerobically on acetate and nitrate. *J Gen Microbiol* 132:3179–3185.
- Korotkova N, Chistoserdova L, Lidstrom ME (2002) Poly-beta-hydroxybutyrate biosynthesis in the facultative methylotroph *Methylobacterium extorquens* AM1: Identification and mutation of gap11, gap20, and phaR. *J Bacteriol* 184:6174–6181.
- Korotkova N, Chistoserdova L, Kuksa V, Lidstrom ME (2002) Glyoxylate regeneration pathway in the methylotroph *Methylobacterium extorquens* AM1. *J Bacteriol* 184:1750–1758.
- Alber BE, Spanheimer R, Ebenau-Jehle C, Fuchs G (2006) Study of an alternate glyoxylate cycle for acetate assimilation by *Rhodobacter sphaeroides*. *Mol Microbiol* 61:297–309.
- Meister M, Saum S, Alber BE, Fuchs G (2005) L-malyl-coenzyme A/beta-methylmalyl-coenzyme A lyase is involved in acetate assimilation of the isocitrate lyase-negative bacterium *Rhodobacter capsulatus*. *J Bacteriol* 187:1415–1425.
- Erb TJ, et al. (2007) Synthesis of C5-dicarboxylic acids from C2-units involving crotonyl-CoA carboxylase/reductase: The ethylmalonyl-CoA pathway. *Proc Natl Acad Sci USA* 104:10631–10636.
- Hacking AJ, Quayle JR (1974) Purification and properties of malyl-coenzyme A lyase from *Pseudomonas* AM1. *Biochem J* 139:399–405.
- Massou S, Nicolas C, Letisse F, Portais JC (2007) Application of 2D-TOCSY NMR to the measurement of specific  $^{13}\text{C}$ -enrichments in complex mixtures of  $^{13}\text{C}$ -labeled metabolites. *Metab Eng* 9:252–257.
- Massou S, Nicolas C, Letisse F, Portais JC (2007) NMR-based fluxomics: Quantitative 2D NMR methods for isotopomers analysis. *Phytochemistry* 68:2330–2340.
- Berg IA, Kockelkorn D, Buckel W, Fuchs G (2007) A 3-hydroxypropionate/4-hydroxybutyrate autotrophic carbon dioxide assimilation pathway in Archaea. *Science* 318:1782–1786.
- Kniemeyer O, et al. (2007) Anaerobic oxidation of short-chain hydrocarbons by marine sulphate-reducing bacteria. *Nature* 449:898–901.
- Boll M, Fuchs G, Heider J (2002) Anaerobic oxidation of aromatic compounds and hydrocarbons. *Curr Opin Chem Biol* 6:604–611.
- Crowther GJ, Kosaly G, Lidstrom ME (2008) Formate as the main branchpoint for methylotrophic metabolism in *Methylobacterium extorquens* AM1. *J Bacteriol* 190:5057–5062.
- Van Dien SJ, Lidstrom ME (2002) Stoichiometric model for evaluating the metabolic capabilities of the facultative methylotroph *Methylobacterium extorquens* AM1, with application to reconstruction of C(3) and C(4) metabolism. *Biotechnol Bioeng* 78:296–312.
- Wiechert W, Moloney M, Petersen S, de Graaf AA (2001) A universal framework for  $^{13}\text{C}$  metabolic flux analysis. *Metab Eng* 3:265–283.